Journal of Medicinal and Nanomaterials Chemistry, 2019, 1(2), 186-190.

FULL PAPER

Synthesis, Characterization and Optical Properties of Co_3O_4 Nanoparticles

Aliakbar Dehno Khalaji *

Department of Chemistry, Faculty of Science, Golestan University, Gorgan, Iran

Received: 11 Februry 2018, Revised: 24 February 2018 and Accepted: 13 March 2018.

ABSTRACT: Mononuclear acyclic cobalt(II) complex [Co**L**]$(NO_3)_2$, with the L = 3,3′-dimethoxy-2,2′-(propane-1,3-diyldioxy)dibenzaldehyde was synthesized and used as a precursor for preparation of the Co_3O_4 nanoparticles. The method was based on thermal decomposition of the cobalt(II) complex at 450 ºC for 3 h in air atmosphere. The cobalt oxide nanoparticles were characterized using FT-IR, UV-Vis, XRD, SEM, and TEM techniques. The FT-IR and XRD results revealed that the Co_3O_4 nanopartcles were pure cubic and single phase. TEM image proved the formation of weakly agglomerated Co_3O_4 consisted of uniformaly shaped nanoparticles. The average particle size of the obtained Co_3O_4, derived from transmission electron microscopy data was approximately 17 nm, which is in agreement with that calculated by XRD. In addition, the optical spectrum indicated one direct band gap at 2.3 eV.

KEYWORDS: Cobalt(II) complex, Co_3O_4 nanoparticles, Thermal decomposition, Optical properties

GRAPHICAL ABSTRACT:

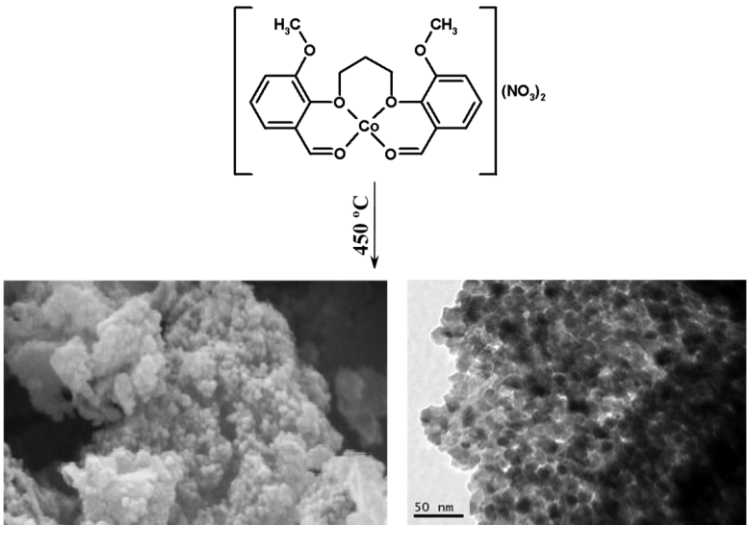

1. Introduction

Recently, research into spinel-type cobalt oxide (Co_3O_4) [1-7] as a p-type semiconducting materials, has increased much attention in the various fields such as lithium-ion batteries [2-4], heterogeneous catalysis [5-7], high-performance supercapacitors[8], and gas sensing properties [9]. Among the various transition metal oxides, Co_3O_4 has a wide range of applications [10-12]. Various methods including, solid-state thermal decomposition [13-20], solvo- [21-23] and hydro-thermal [24-27] and chemical precipitation [28] have been reported for synthesis of the Co_3O_4. Among these techniques, solid-state thermal decomposition method was found to be simple, easy, low cost, and without

*Corresponding author: Aliakbar Dehno Khalaji, Email: E-mail: alidkhalaji@yahoo.com , ad.khalaji@gu.ac.ir , Tel: 0098-17- 32245882; Fax: 0098-17-32245882

Journal of Medicinal and Nanomaterials Chemistry

usage solvent or surfactant [13-20]. In our group, we have been interested in the synthesis and characterization of the Co_3O_4 nanoparticles [29,30]. Herein, I reported the rapid and simple synthesis of Co_3O_4 nanoparticles via solid state thermal decomposition of acyclic cobalt(II) complex (Scheme 1).

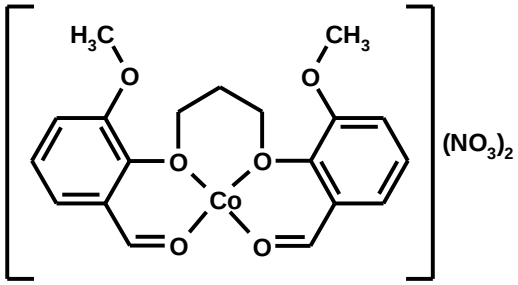

Scheme 1. Chemical structure of acyclic cobalt(II) complex

2. Materials and Methods

All reagents and solvents for synthesis and analysis were commercially available and used as received without further purifications. 1,2-bis(2-formyl-3-methoxyphenyl)propane (**L**), used in the synthesis was prepared by the reaction of 3-methoxysalicylaldehyde and 1,3-dibromopropane in the presence of K_2CO_3 at 80 ºC according to the literature [31]. The elemental analysis was carried out using a Heraeus CHN-O-Rapid analyzer, and the results agreed with the calculated values. Optical absorption spectra were recorded on a Cary 100 UV-Visible Spectrophotometer, VARIAN EL 12092335 in a wavelength ranging from 200 nm to 700 nm at the room temperature. The sample for UV-Vis studies was well dispersed in distilled water by sonication for 10 min to form a homogeneous suspension. X-ray powder diffraction (XRD) pattern of the complex was recorded using a Bruker AXS diffractometer D8 ADVANCE with Cu-Kα radiation with nickel beta filter in the range $2\theta = 10^o–80^o$. Fourier transform infrared spectra were recorded as a KBr disk on a FT-IR Perkin–Elmer spectrophotometer. The transmission electron microscopy (TEM) images were obtained using a JEOL JEM 1400 TEM with an accelerating voltage of 120 kV. The scanning electron microscopy (SEM) images were taken using a Philips XL-30 ESEM. The TEM samples were prepared by dispersing the powder in ethanol by ultrasonic vibration.

A methanolic solution of $Co(NO_3)_2{\cdot}6H_2O$ (2 mmol) was added dropwise to a solution of **L** (2 mmol) in MeOH (50 mL), and the reaction mixture was stirred for 2 h. The microcrystalline powders were filtered, washed with water and dried in air. *Anal*. calcd for $C_{19}H_{24}O_{14}N_2Co$: C, 40.51; H, 4.30; N, 4.97%; Found C, 40.36; H, 4.25; N, 5.06%. FT-IR (KBr, cm^{-1}): 3012, 2941 (C-H), 2856 (-CH=O), 1692 (C=O), 1583, 1484, 1441 (C=C aromatic), 1383 (NO_3).

0.5 g of cobalt(II) complex was loaded into a platinum crucible, placed in an electric furance and heated up to 450ºC for 3.5 h. The resulting black product was collexted, washed with ethanol to remove eventual impurities and dried in air. FT-IR (KBr pellet, cm^{-1}): 3377, 1625 (H_2O), 663, 566 (Co-O).

3. Results and Discussion

FT-IR spectrum of cobalt(II) complex showed several bands at 3394, 2856, 1692 and 1383 cm^{-1} due to the ν(-OH), ν(-HC=O), ν(-C=O) and ν(NO_3), respectively [32,33]. In particular, these peaks disappeared in the the FT-IR spectrum of Co_3O_4 nanoparticles (Figure 1). FT-IR spectrum of Co_3O_4 contained two strong absorption bands at 566 cm^{-1} and 663 cm^{-1} due to ν(Co^{III}-O) and ν(Co^{II}-O) vibrations, which confirm the successful preparation of Co_3O_4 nanoparticles as spinel structure [33,34]. These bands confirmed that the Co(II) and Co(III) were tetrahedrally and

Journal of Medicinal and Nanomaterials Chemistry

octahedrally coordinated, respectively [13]. In addition, the two broad peaks observed at 3377 and 1625 cm^{-1} should be assigned to –OH vibration modes of water molecules which adsorbed on the surface of Co_3O_4 nanoparticles [33, 34].

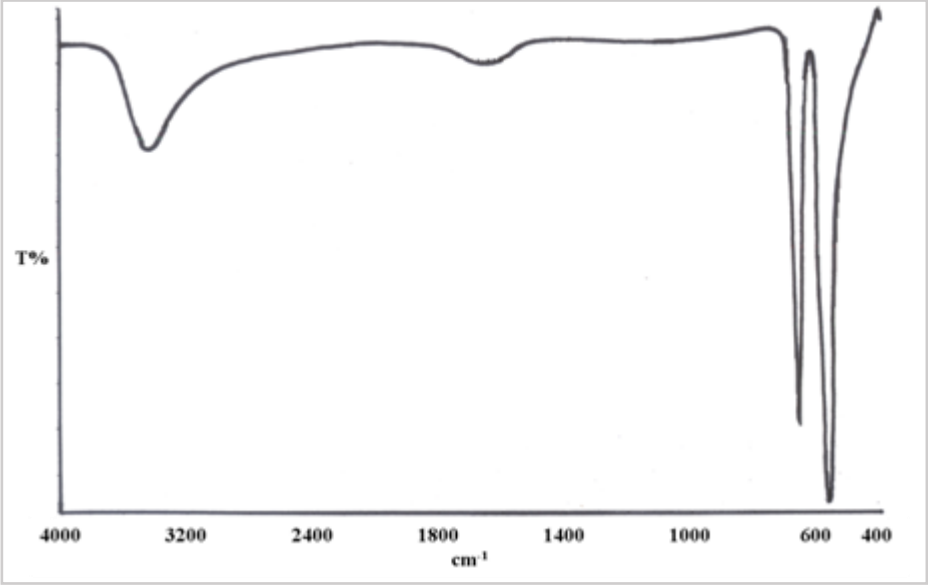

Fig.1. FT-IR spectrum of Co_3O_4 nanoparticles.

The morphology of the Co_3O_4 naoparticles was considered by SEM and TEM. As shown in Figure 2 the Co_3O_4 nanoparticles found in an plate-like shape with weak agglomeration. Also, the average particle size was found to be 17 nm. However, the SEM and TEM images revealed that the shape of the particles was regular and uniform with a narrow size distribution.

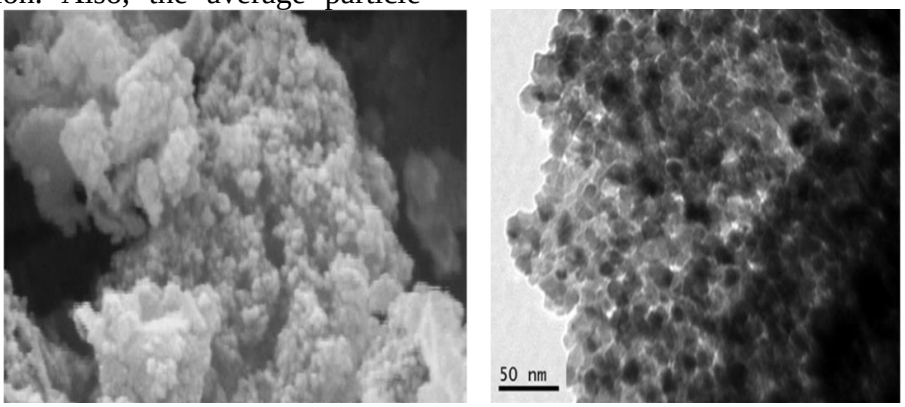

Fig.2. SEM (left) and TEM (right) images of Co_3O_4 nanoparticles.

XRD pattern of Co_3O_4 nanoparticles in (Fig. 3) indicates the purity of the product. The diagram of the Co3O4 in $10^{o} \leqq 2\theta \leqq 80°$, presents all the lines of magnetite (JCPDS No. 42-1467) and their intensities match the theoretical values [33, 34]. No distinct diffraction peak for other cobalt oxides was observed. The average particle size calculated using Scherrer equation, according to the (311) diffraction peak at $2\theta \approx 37$, was about 17 nm.

UV-vis absorbance spectrum (Figure 4) of the Co_3O_4 nanoparticles shows two absorption bands in the 250 and 535 nm due to the LMCT transitions ($O^{2-} \rightarrow Co^{2+}$ and $O^{2-} \rightarrow Co^{3+}$) with a small red shift in comparison with the other reports [35]. The direct band gap energy of Co_3O_4

Journal of Medicinal and Nanomaterials Chemistry

nanoparticles is 2.3 eV and is higher than the bulk (1.6 eV) [35].

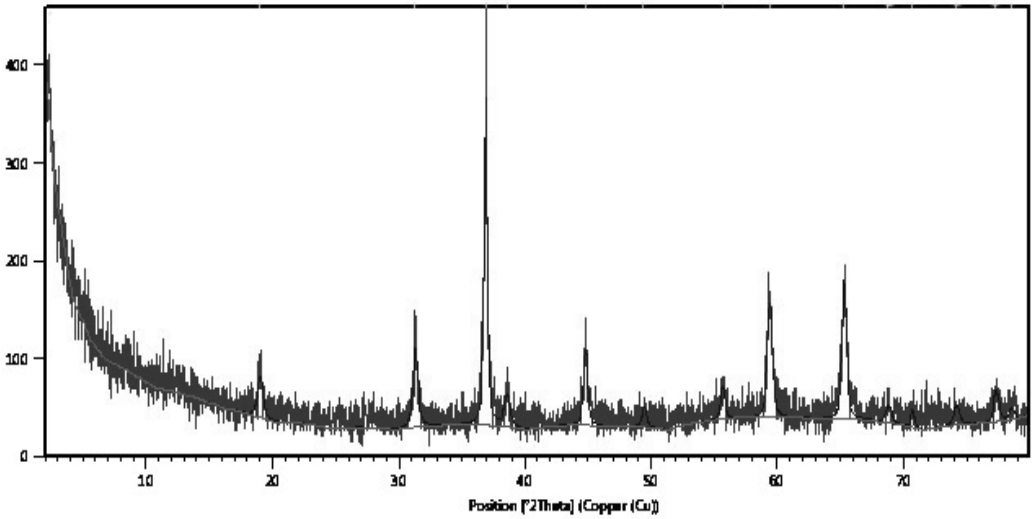

Fig. 3. XRD pattern of Co_3O_4 nanoparticles.

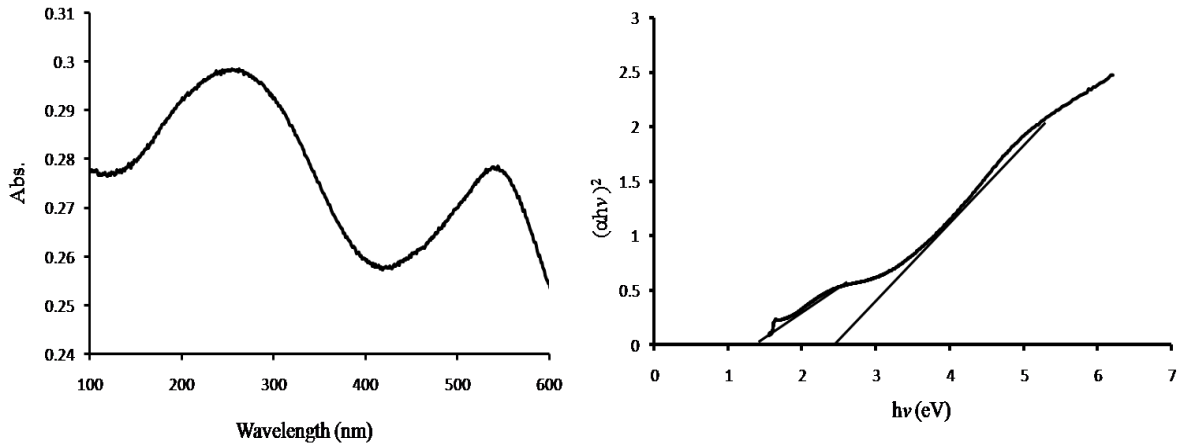

Fig. 4. UV-Vis spectrum (Left) and $(\alpha h\nu)^2 \approx h\nu$ curve (right) of Co_3O_4 nanoparticles.

4. Conclusions

In this research studry, an easy, rapid, simple and low-cost method was employed to synthesize the spinel Co_3O_4 nanoparticles *via* solid state thermal decomposition of the mononuclear acyclic cobalt(II) complex [Co**L**]$(NO_3)_2$. According to the results of the SEM and TEM analysis, uniform and cubic-like Co_3O_4 nanoparticles with weak agglomeration was obtained. XRD and FT-IR confirmed the formation of the pure and single highly crystalline Co_3O_4 phase. Also, the optical absorption band gap was estimated 2.3 eV.

Acknowledgments

The financial support from the Golestan University is gratefully acknowledged.

References

1. Zhao C, Huang B, Zhou J, Xie E (**2014**) Phys. Chem. Phys., **16**:19327-19332.
2. Jin L, Li X, Ming H, Wang H, Jia Z, Fu Y, Adkins J, Zhou Q, Zheng J (**2014**) RSC Adv, **4**:6083-6089.
3. Wen W, Wu JM, Cao MH (**2014**) Nanoscale, **6**:12476-12481.

Journal of Medicinal and Nanomaterials Chemistry

4. Su P, Liao S, Rong F, Wang F, Chen J, Li C, Yang Q (**2014**) J. Mater. Chem. A, **2**:17408-17414.
5. Teng Y, Song LX, Wang LB, Xia J (**2014**) J. Phys. Chem. C., **118**:4767-4773.
6. Wang J, Qiao Z, Zhang L, Shen J, Li R, Yang G, Nie F (**2014**) Cryst. Eng. Commun., **16**:8673-8677.
7. Roy M, Ghosh S, Naskar MK (**2014**) Dalton. Trans., **43**:10248-10257.
8. Meher SK, Rao GR (**2011**) J. Phys. Chem. C., **115**:25543-25556.
9. Dou Z, Cao C, Chen Y, Song W (**2014**) Chem. Commun., **50**:14889-14891.
10. Sahoo P, Djieutedjeu H, Poudeu PFP(**2013**) J. Mater. Chem. A., **1**:15022-15030.
11. Farhadi S, Pourzare K, Bazgir S (**2014**) J. All. Compd., **587**:632-637.
12. Ghiasi M, Malekzadeh A, Mardani H (**2016**) Mater. Sci. Sem. Proces., **42**:311-318.
13. Khansari A, Salavati-Niasari M, Kazemio Babaheydari A (**2012**) J. Clust. Sci. **23**:557-565.
14. Salavati-Niasari M, Davar F, Mazaheri M, Shaterian M (**2008**) J. Mag. Mag. Mater. **320**:575-578.
15. Hosny NM (**2014**) Mater. Chem. Phys., **144**:247-251.
16. Pal J, Chauhan P (**2010**) Mater. Charact., **61**:575-579.
17. Fan S, Liu X, Li Y, Yan E, Wang C, Liu J, Zhang Y (**2013**) Mater. Lett., **91**:291-293.
18. Wang R.-T, Kong L.-B, Lang J.-W, Wang X.-W, Fan S.-Q, Luo Y.-C, Kang L (**2012**) J. Power. Sourc. **217**:358-363.
19. Hosseinian A, Jabbari S, Rahimipour HR, Mahjoub AR (**2012**) J. Mol. Struct., **1028**:2215-221.
20. Farhadi S, Pourzare K (**2012**) Mater. Res. Bull., **47**:1550-1556.
21. Wang L, Deng J, Lou Z, Zhang T (**2014**) Sensors. Actuators. B., **201**:1-6.
22. Jin Y, Wang L, Shang Y, Gao J, Li J, He X (**2015**) Electrochim. Acta., **151**:109-117.
23. Huang Y, Chen C, An C, Xu C, Xu Y, Wang Y, Jiao L, Yuan H (**2014**) Electrochim. Acta., **145**:34-39.
24. Teng Y, Yamamoto S, Kusano Y, Azuma M, Shimakawa Y (**2010**) Mater. Lett., **64**:239-242.
25. Hashemi Amiri SE, Vaezi MR, Kandjani AE (**2011**) J. Cer. Process. Res., **12**:327-331.
26. Ren M, Yuan S, Su L, Zhou Z (**2012**) Solid. State. Sci., **14**:451-455.
27. Liu Y, Zhang X, Wu Y (**2011**) Mater. Chem. Phys., **128**:475-482.
28. Makhlouf SA, Bakr ZH, Aly KI, Moustafa MS (**2013**) Superlat. Microstruct., **64**:107-117.
29. Khalaji AD, Nikookar M, Fejfarova K, Dusek M (**2014**) J. Mol. Struct., **1071**:6-10.
30. Khalaji AD (**2015**) J. Appl. Chem. Res., **9**:41-45.
31. Khalaji AD, Rahdari R, Gharib F, Sanmartín Matalobos J, Das D (**2015**) J. Cer. Proc. Res., **16**:486-489.
32. Shen SF, Xu ML, Lin DB, Pan HB (**2017**) App. Surf. Sci., 396:327-332.
33. Farhadi S, Safabakhsh J (**2012**) J. All. Compd., **515**:180-185.
34. Salavati-Niasari M, Mir N, Davar F (**2009**) J. Phys. Chem. Sol., **70**:847-852.
35. Sharma JK, Srivastava P, Singh G, Shaheer Akhtar M, Ameen S (**2015**) Mater. Sci. Eng. B., **193**:181-188.

How to cite this manuscript: Fatemeh Houshmand *, Hamide Neckoudari and Majid Baghdadi. Host-guest interaction in chitosan– MX (3-chloro-4-(dichloromethyl)-5-hydroxy-2(5H)-furanone) complexes in water solution: Density Functional Study. Journal of Medicinal and Nanomaterials Chemistry, 2019, **1**(2) , 186-190.